GA–A24346

A COMPARISON OF SAWTEETH IN BEAN AND OVAL SHAPED PLASMAS

by
E.A. LAZARUS, M.E. AUSTIN, K.H. BURRELL, M.S. CHU, A.W. HYATT,
R.J. JAYAKUMAR, T.C. LUCE, M.A. MAKOWSKI, T.H. OSBORNE,
C.C. PETTY, P.A. POLITZER, R. PRATER, H. REIMERDES, J.T. SCOVILLE,
M.R. WADE, and F.L. WAELBROECK

JULY 2003

DISCLAIMER

GA–A24346

A COMPARISON OF SAWTEETH IN BEAN AND OVAL SHAPED PLASMAS

by

E.A. LAZARUS,* M.E. AUSTIN,† K.H. BURRELL, M.S. CHU, A.W. HYATT, R.J. JAYAKUMAR,‡ T.C. LUCE, M.A. MAKOWSKI,‡ T.H. OSBORNE, C.C. PETTY, P.A. POLITZER, R. PRATER, H. REIMERDES,$^{\Delta}$ J.T. SCOVILLE, M.R. WADE,* and F.L. WAELBROECK†

This is a preprint of a paper to be presented at the 30th European Physical Society Conference on Controlled Fusion and Plasma Physics, St Petersburg, Russia, July 7–11, 2003 and to be published in the *Proceedings.*

*Oak Ridge National Laboratory, Oak Ridge, Tennessee.

†University of Texas – Austin, Austin, Texas.

‡Lawrence Livermore Natonal Laboratory, Livermore, California.

$^{\Delta}$Columbia University, New York, New York.

Work supported by the U.S. Department of Energy under Contract Nos. DE-AC05-00OR22725, DE-AC03-99ER54463, W-7405-ENG-48, DE-FG03-97ER54415, and DE-FG02-89ER53297

GENERAL ATOMICS PROJECT 30033

JULY 2003

A Comparison of Sawteeth in Bean and Oval Shaped Plasmas

E.A. Lazarus[1], M.E. Austin[2], K.H.Burrell[3], M.S. Chu[3], A.W. Hyatt[3], R.J. Jayakumar[4], T.C. Luce[3], M.A. Makowski[4], T.H. Osborne[3], C.C. Petty[3], P.A. Politzer[3], R. Prater[3], H. Reimerdes[5], J.T. Scoville[3], M.R.Wade[1], and F.L. Waelbroeck[2]

[1]*Oak Ridge National Laboratory, P.O. Box 2008, Oak Ridge, Tennessee 37831*
[2]*University of Texas, Austin, Texas 87812*
[3]*General Atomics, P.O. Box 85608, San Diego, California 92186-5608*
[4]*Lawrence Livermore National Laboratory, P.O. 808, Livermore, California 94551*
[5]*Columbia University, New York, New York USA*

A set of experiments has been conducted in DIII–D to compare sawteeth in bean and oval shaped, inner-wall limited plasmas. The distinction is that the oval will violate the ideal Mercier criterion with q_0 somewhat above 1, while a low κ bean shape will remain ideally Mercier stable with q_0 somewhat below 1. In this way we hope to separate the roles of internal kink and interchange in the behavior of sawteeth. The experimental arrangement allows us to change shape on successive discharges, which helps minimize systematic errors in the data. The principal diagnostics are motional Stark effect for the internal poloidal field, electron cyclotron emission for electron temperature, multi-pulse Thomson scattering for the density profile, and charge exchange recombination (CER) for ion temperature and toroidal velocity. New CER channels with greatly improved signal-to-noise allow resolution of the ion behavior during a sawtooth. These channels are critical to our ability to resolve the evolution of the ion temperature profiles during the sawteeth, enabling transport analysis. The experimental conditions are constant for about 3 s with 2.5 MW of neutral beam heating, which is needed for the diagnostics. The plasma shape is grown during the current ramp-up to facilitate equilibration of the current profile, which is stationary (aside from the sawteeth) as are temperature and density profiles. In some cases ECH heating is added. This increases the electron temperature so it is nearly equal to the ion temperature.

At the present time the calibration of the MSE diagnostic calibration is incomplete and we will avoid analysis that is dependent on accurate knowledge of the equilibrium. After a brief characterization of the global features of the discharges, this paper will focus on two aspects of the experiment. There are two principal observations reported here. First, the nature of the sawtooth collapse in the two shapes, which we believe to be a current-driven instability in the oval and a pressure-driven instability in the bean. Second, the differences in the ion response to m/n=1/1 activity relative to the electron response and furthermore how this difference is affected by the plasma shape.

The general conditions (Fig. 1) are established principally to satisfy mutually a set of conditions: 1) consistency with coil and power supply limits, 2) ECH resonance near the center of the plasma, 3) several ECE diagnostic channels outside the inversion radius, 4) high quality MSE signal, and 5) shapes consistent with a single configuration of poloidal field power supplies so the shape may be switched between the two on alternate shots. The latter is to minimize any systematic errors in measurements. The plasma radius is increased during the current ramp to promote rapid equilibration of the current profile. An early heating beam is operated from 500 to 1700 ms to assure that the discharge evolves in a very regular way and there will not be any problem with locked modes. For simplicity we have chosen to make inside-limited L-mode plasmas. The principal beam begins at 1700 ms and continues to 5000 ms. The data interval is 2000 to 5000 ms and during this interval the sawteeth are extremely reproducible; aside from the sawtooth perturbation the MSE pitch angle is constant during the data interval.

Typical results are shown in Fig. 2 for the bean and oval shapes. Central T_e shows the regularity of the sawteeth. T_i at R=1.77 m is not at the same spatial location as T_e in this figure. In both cases $T_i > T_e$ as well as the sawtooth amplitudes, $\Delta T_i > \Delta T_e$. (For these conditions the integrated beam power to ρ=0.5 is about 7/5 ions to electrons.) The dB/dt signal makes the distinction that there is a growing precursor oscillation (m/n=1/1) in the oval but virtually no precursor in the bean. Instead there is a large post-cursor oscillation. In both cases the average pitch angle of the vertical field is constant. In the bean a modulation with the sawtooth is observed, but not in the oval. The sawtooth period is about 120 ms in the bean and half that in the oval and does not correlate with the energy confinement times, which are quite similar. There is a discrete loss of about 15% of the total plasma energy on each sawtooth collapse in the bean but no noticeable loss in the oval. The neutron signal shows a sawtooth waveform indicating that the fast ions are spilled from the core on each sawtooth collapse in both shapes. This completes our description of gross phenomenology.

	Oval	Bean
Shot	113915	113920
R_{out} (m)	1.640	1.645
Z_{out} (m)	0.002	0.005
a (m)	0.624	0.629
elong	1.636	1.516
utri	0.091	0.520
indent	0.000	0.070
V (m^3)	19.980	17.535
A (m^2)	1.972	1.778
W (MJ)	0.244	0.242
β_T (%)	0.591	0.674
β_p	0.448	0.211
Li	1.411	1.236
q_{95}	5.360	3.929
I_p (MA)	0.897	1.385
$B_T(0)$ (T)	-1.801	-1.798
$\langle n_e \rangle$ ($\times 10^{19}$)	1.850	2.009

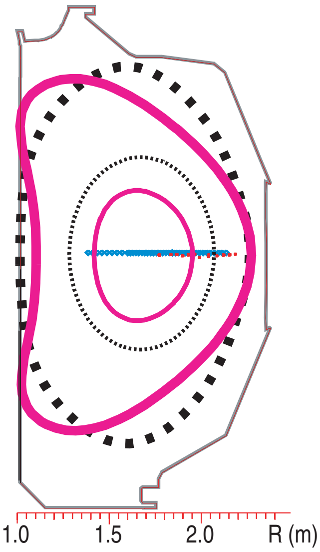

Fig. 1. The bean and oval shapes, and plasma parameters of this experiment. The inner surfaces are inversion radii. The red markers are CER measurement locations and the blue diamonds are ECE measurement location.

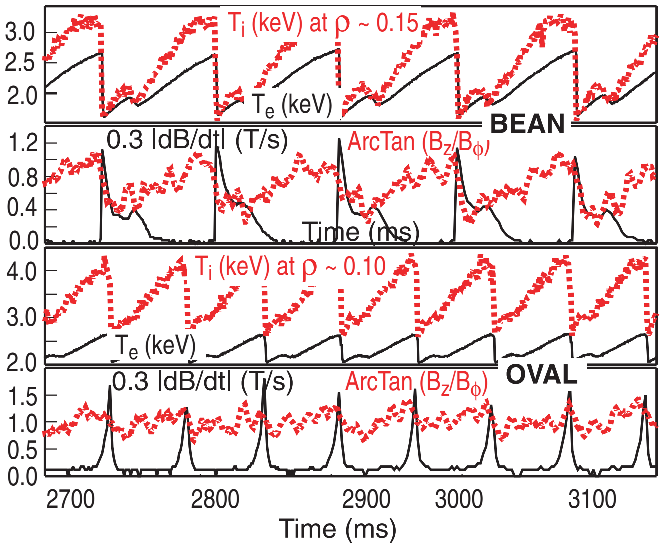

Fig. 2. Sawteeth in bean and oval shapes. T_e, T_i, $|dB_\varphi/dt|$, and magnetic field pitch angle at R=1.68 m are shown.

We now turn our attention to the sawtooth collapse. The ECE diagnostic has 10 µs resolution and the m/n=1/1 frequency is in the range 7.5 to 10.5 kHz depending on the type of sawtooth and the phase in the sawtooth event. The primary analysis tools are a visual presentation of the ECE data that gangs together a color map, a contour plot, a time plot at a selectable radius and a radial plot at selectable time. By sliding the cursor one gets a very good visual of the reconnection process in 10 μs steps. For ECE radius we are using the vacuum field radius. The second tool is the cross correlation of the ECE signals with an outer magnetic probe that is dominated by the n=1 signal (actually the difference of two probes separated by 180° in toroidal angle). From this we get the phase relationship of the radial channels along with the coherence of the channels with the magnetic perturbation. As is seen in Fig. 3, the oval has a rotating structure prior to the collapse. The bean shows no such structure, but a rotating structure appears immediately after the collapse. In the oval, the interval 2 ms prior to the sawtooth crash at 3443.15 the cross correlation shows a 180°phase jump characteristic of an island at 1.45 m. Cross correlation in the 2 ms after the crash simply show low coherence and no detectable structure. The midplane profile shows a flattening at this same location that oscillates from inside to outside the magnetic axis. Turning to the bean, we examine the sawtooth at 3360.7 ms. In the interval 2 ms before the sawtooth crash, there is no visible indication of a crash and correlation analysis does not indicate the presence of an island. Rather, the cross correlation shows low coherence. In the 2 ms interval after, correlation analysis shows phase jumps characteristic of an island at 1.85 m and a second at 1.94 m. The island corresponding to the phase jump at 1.85 m, is seen with opposite phase at 1.35 ms. However 40 ms later only a single island is observed at R = 1.8 m. As the n=1 amplitude is dying away at this later time, we know the mode is decaying. The reconnection event at the time of the collapse is best observed in the T_e contour plots. The oval shows an event occurring over 80 μs. In the bean the collapse is faster with the high-pressure core being expelled within a time interval of 40 μs. In the oval the final state has the T_e profile completely flattened, in the bean there is perhaps a degree of hollowness in the final T_e profile. The sawtooth events in the oval are rather traditional in that there is an island of increasing size and surrounding a hot core. The instability grows and overtakes the core in the reconnection event. The bean does not have these features, but rather the T_e profile is stationary in shape. The amplitude increases until there is an explosive expulsion of the hot core followed by a strongly helical state. It is not possible to say there is no magnetic precursor to this expulsion. However, if there is a small magnetic precursor, it exists for less than 40 μs, much less than a toroidal transit time. In both cases the ion sawtooth is larger than the electron sawtooth. In summary, the oval has an observable island before the collapse that grows to, what appears to be, a total reconnection at the collapse. The energy from the core is spread through the plasma volume but none appears lost across the boundary. This appears to be a Kadomdtsev-like process. In the bean, by contrast, we see no evidence of an island before the collapse.

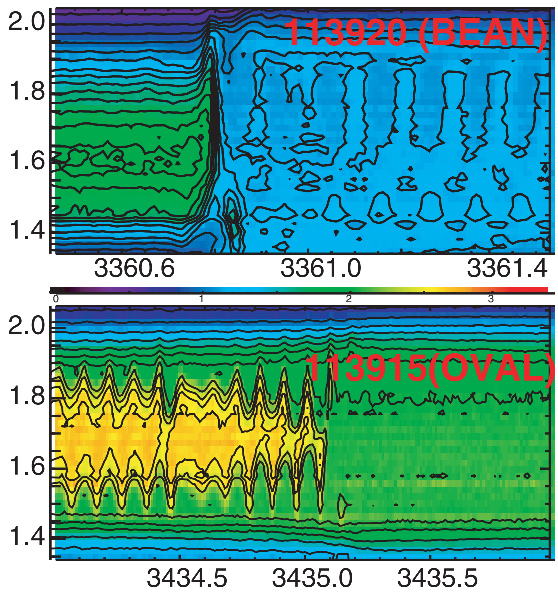

Fig. 3. Color map of T_e from ECE showing the reconnection events in radius-time space. The color bar is 0–3.5 keV.

Rather an explosive growth without precursor in which the hot core is violently expelled, with some of the energy lost across the last closed surface. The plasma reconnects to a state with strong helicity and a double island structure. For these reasons we interpret these, respectively, as current-driven (oval) and pressure-driven (bean) instabilities.

Further analysis is required to know how well we have satisfied the premise of the experiment, moving the Mercier limit away from the q=1. In particular the q profile must be known precisely. Nevertheless, the results are surprising. We had expected to violate the Mercier criterion in the oval and see that the plasma could not hold pressure when q was still above 1. We might have expected just the opposite result, no visible precursor for the oval and strong precursor oscillations in the bean which should retain pressure for q<1.

We now turn to the ion behavior within the sawtooth period. The ion data we are using has already been presented in Fig. 2. The data channels for the CER diagnostic extend into a radius R= 1.77 m. In Fig. 4 we display this R=1.77 m channel and the ECE channel at the same radius. The ECE signal is stretched and shifted vertically to best overlay the ion sawteeth. The T_e range at this radius is 1.08–1.52 keV in the oval and 1.34–1.68 keV in the bean (no ECH). In the oval shape, the partial reconnection seen in the electron channel is visible in the ions. In the bean the ions experience the partial reconnection but they recover and begin reheating *before* the electrons. At the top of the sawtooth in the oval the temporal behavior of T_e and T_i are similar, while in the bean T_i begins to rollover while T_e is still rising. These effects are more pronounced at larger radii, closer to the inversion radius. These distinctions are more visible in the toroidal rotation than in T_i. In summary, the response of the ions to m/n=1/1 activity differs from the electron response and these differences depend on the plasma shape. The sawtooth collapse appears to occur at the same time in both channels, although the T_i data at the highest time resolutions is not yet analyzed.

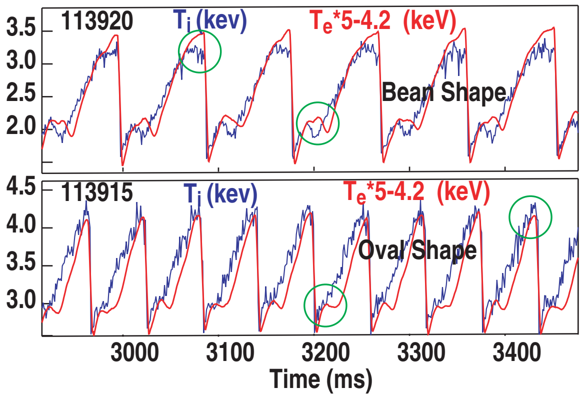

Fig. 4. T_e and T_i waveforms at R=1.77 m in oval and bean shapes.

Work supported by U.S. Department of Energy under Contracts DE-AC05-00OR22725, DE-AC03-99ER54463, W-7405-ENG-48, and Grants DE-FG03-97ER54415 and DE-FG02-89ER53297.